Heart Failure with Preserved Ejection Fraction:

Franssen, C.P.M.

2017

document version
Publisher's PDF, also known as Version of record

Chapter 3

Myocardial Microvascular Inflammatory Endothelial Activation in Heart Failure with Preserved Ejection Fraction

Franssen C*, Chen S*, Unger A, Korkmaz HI, De Keulenaer GW, Tschöpe C, Leite-Moreira AF, Musters R, Niessen HW, Linke WA, Paulus WJ, Hamdani N.

*Authors contributed equally

JACC Heart Fail. 2016;4;312-24.

Editorial comment:
Inflammation in Heart Failure With Preserved Ejection Fraction: Time to Put Out the Fire.
Gomberg-Maitland M, Shah SJ, Guazzi M
JACC Heart Fail. 2016;4:325-8.

Myocardial Microvascular Inflammatory endothelial activation in Heart Failure with Preserved Ejection Fraction

By

Constantijn Franssen*[1], M.D., Sophia Chen*[1], B.Sc., Andreas Unger[2],Ph.D., H. Ibrahim Korkmaz[1,3], M.Sc., Gilles W. De Keulenaer[4], M.D., Ph.D., Carsten Tschöpe[5], M.D., Ph.D., Adelino F. Leite-Moreira[6], M.D., Ph.D., René Musters[1], Ph.D., Hans W.M. Niessen[3], M.D., Ph.D., Wolfgang A. Linke[2], Ph.D., Walter J. Paulus[1], M.D., Ph.D. and Nazha Hamdani[1,2],Ph.D.

From

[1]Department of Physiology, Institute for Cardiovascular Research, VU University Medical Center, Amsterdam, The Netherlands,
[2]Department of Cardiovascular Physiology, Ruhr University Bochum, Germany,
[3]Department of Pathology and Cardiac Surgery VU University Medical Center, Amsterdam, The Netherlands
[4]Laboratory of Physiology, University of Antwerp, Belgium,
[5]Department of Cardiology and Pneumology, Charité – Universitätsmedizin Berlin, Berlin, Germany,
[6]Department of Physiology and Cardiothoracic Surgery, University of Porto, Portugal,

* C.F. and S.C. equally contributed to this manuscript

Short title: Microvascular endothelial inflammation in HFpEF

ABSTRACT

Background - Metabolic risk is associated with diastolic LV dysfunction and heart failure with preserved ejection fraction (HFpEF).
Objectives - The present study investigates if systemic, low-grade inflammation of metabolic risk contributes to diastolic LV dysfunction and HFpEF through coronary microvascular endothelial activation, which alters paracrine signalling to cardiomyocytes and predisposes them to hypertrophy and high diastolic stiffness.
Methods - We explored inflammatory endothelial activation and its effects on oxidative stress, NO bioavailability and cGMP-PKG signalling in myocardial biopsies of HFpEF patients and validated our findings by comparing obese ZSF1-HFpEF rats to ZSF1-Control (Ctrl) rats.
Results - In myocardium of HFpEF patients and ZSF1-HFpEF rats we observed: 1) E-selectin and ICAM-1 to be upregulated, 2) NOX2 expression to be raised in macrophages and endothelial cells but not in cardiomyocytes and 3) uncoupling of eNOS which was associated with reduced myocardial nitrite/nitrate concentration, cGMP-content and PKG-activity.
Conclusions - HFPEF is associated with coronary microvascular endothelial activation and oxidative stress. This leads to a reduction of NO-dependent signalling from endothelial cells to cardiomyocytes, which can contribute to the high cardiomyocyte stiffness and hypertrophy observed in HFPEF.

CONDENSED ABSTRACT

The present study investigates if systemic, low-grade inflammation of metabolic risk contributes to HFpEF through coronary microvascular endothelial activation. Inflammatory endothelial activation, myocardial oxidative stress, NO bioavailability and cGMP-PKG signalling were investigated in human HFpEF myocardial biopsies and in obese ZSF1-HFpEF rats. Endothelial E-selectin and ICAM-1 were upregulated. NOX2 expression was raised in macrophages, but not in cardiomyocytes and 3-Nitrotyrosine expression was limited to endothelial cells. Myocardial eNOS was uncoupled and associated with reduced myocardial nitrite/nitrate concentration, cGMP-content and PKG-activity. Metabolic risk therefore contributes to HFpEF development through myocardial microvascular inflammation, which alters NO signalling from endothelial cells to cardiomyocytes.

KEYWORDS

Heart failure, inflammation, nitric oxide, endothelium, oxidative stress

ABBREVIATIONS

AS: aortic stenosis
cGMP: cyclic guanosine monophosphate
DM: diabetes mellitus
eNOS: endothelial nitric oxide synthase
HFpEF: heart failure with preserved ejection fraction
HFrEF: heart failure with reduced ejection fraction
ICAM-1: Intercellular Adhesion Molecule 1
NO: nitric oxide
NOX2: NADPH oxidase 2
PKG: protein kinase G

INTRODUCTION

Metabolic risk is increasingly recognized as an important contributor to diastolic left ventricular (LV) dysfunction and to heart failure with preserved ejection fraction (HFpEF). Recent longitudinal non-invasive studies over a 4 year time interval revealed close correlations between diastolic LV stiffness and body mass index (BMI) (1,2). These studies concluded that weight loss and reduction of central adiposity could prevent diastolic LV dysfunction and eventual HFpEF development. Similar evidence was already provided by the All-HAT trial, which enrolled patients with arterial hypertension and one additional cardiovascular risk factor, and observed a high BMI at enrolment to be the strongest predictor for HFpEF development (3). The latter finding was consistent with the high prevalence of overweight/obesity in large HFpEF outcome trials or registries, which almost uniformly reported a median BMI value of HFpEF patients in excess of 30 kg/m^2. In primates developing diet-induced obesity, endothelial inflammatory activation evident from adhesion molecule expression appears to be the earliest manifestation of vascular damage (4). Endothelial inflammatory activation is associated with microalbuminuria, which was recently shown to be associated with diastolic LV dysfunction (5) and to predict HFpEF development (6). When endothelial inflammatory activation evolves to endothelial dysfunction, vasomotor responses become blunted as evident from a lower reactive hyperemic response (7), which provides both diagnostic and prognostic information in HFpEF (8,9). In HFpEF, endothelial dysfunction also closely relates to worsening of symptoms (10), functional capacity (10) and precapillary pulmonary hypertension (11).

This prominent involvement of metabolic risk and endothelial inflammatory activation recently led to a new paradigm for HFpEF development (12). In accordance to this paradigm, metabolic comorbidities drive LV remodeling and dysfunction in HFpEF through coronary microvascular endothelial inflammation, which alters paracrine signalling from endothelial cells to surrounding cardiomyocytes. Especially the fall in nitric oxide-cyclic guanosine monophosphate–protein kinase G (NO-cGMP-PKG) signalling predisposes cardiomyocytes to hypertrophy development and to high diastolic resting tension. Microvascular endothelial dysfunction as a mechanism of LV remodeling in HFpEF differs from heart failure with reduced ejection fraction (HFrEF), where eccentric LV remodeling results from cardiomyocyte cell death pathways such as accelerated autophagy, apoptosis or necrosis (13). It also differs from aortic stenosis (AS),

where concentric LV remodeling is induced by excessive systolic wall stress (14). To establish the validity of endothelial dysfunction controlling LV remodeling in HFpEF, the current study compared microvascular endothelial inflammatory activation and its effects on myocardial oxidative stress, NO bioavailability and cGMP content in myocardial biopsies of HFpEF, HFrEF and AS patients.

Furthermore, we studied the ability of metabolic risk to induce HFpEF through myocardial microvascular endothelial inflammatory activation in leptin-resistant, obese, hypertensive ZSF1 rats. These rats develop a HFpEF phenotype after 20 weeks, which was evident from elevated LV filling pressures with preserved LV systolic function, increased lung weight because of pulmonary congestion and increased stiffness of isolated myocardial strips (15). At that time, a similar assessment of myocardial microvascular endothelial inflammatory activation and its effects on oxidative stress, NO bioavailability, cGMP content and PKG signalling was performed and compared to age matched lean, hypertensive ZSF1 rats with normal diastolic LV function and no lung congestion.

METHODS

A detailed method section can be found in an Online Supplement.

Human samples

Human HFrEF and HFpEF samples were procured from LV biopsies [HFrEF (N=43) and HFpEF (N=36)]. HFrEF and HFpEF patients were hospitalized for HF and underwent transvascular LV endomyocardial biopsy procurement because of suspicion of an infiltrative or inflammatory cardiomyopathy. Patients were included if significant coronary artery disease (stenosis >50%) was ruled out by angiography and if histological analysis of the biopsy showed no evidence of infiltrative or inflammatory myocardial disease. Patients were classified as HFpEF if LVEF was >50%, LV end diastolic volume index <97 ml/m^2, and LV end-diastolic pressure was >16 mmHg (16). If LVEF was <45%, a patient was classified as HFrEF. AS patients (N=67) had severe AS (mean aortic valve area 0.53±0.04cm^2) without concomitant coronary artery disease. Biopsy specimens from this group were procured from endomyocardial tissue resected from the septum (Morrow procedure) during aortic valve replacement. The local ethics committee approved the study protocol. Written informed consent was obtained from all patients. Control human samples (N=4) were procured from patients with life-threatening

arrhythmias, suspected infiltrative heart disease or myocarditis and a preserved LVEF without coronary artery disease in whom histology ruled out myocarditis or infiltrative pathology. Because of limited availability of human myocardial tissue, histological and biochemical determinations could only be performed in subgroups of patients, randomly selected by blinded investigators.

TABLE 1 Baseline Characteristics and Hemodynamics of Patients

	HFpEF (n = 36)	HFrEF (n = 43)	AS (n = 67)	Control (n = 4)	p Value (HFpEF vs. HFrEF)	p Value (HFpEF vs. AS)
Age, yrs	63.8 ± 2.0	60.0 ± 2.1	65.3 ± 1.6	51 ± 4	0.21	0.57
% of males	56	70	47	25	0.24	0.53
% of hypertension	78	16	58	–	<0.0001	0.07
% of DM	47	30	26	–	0.16	0.047
BMI, kg/m^2	30.4 ± 1.0	27.5 ± 0.8	28.1 ± 0.6	–	0.023	0.031
GFR, ml/min/1.73 m^2	72.9 ± 2.3	73.3 ± 2.7	68.9 ± 18.5	–	0.49	0.2
% of atrial fibrillation	14	33	2	–	0.067	0.028
% taking medications						
ACEI/ARB	81	81	43	–	1.00	<0.0001
Beta-blocker	53	63	61	–	0.49	0.52
Diuretic agent	78	72	54	–	0.61	0.028
Aldosterone receptor antagonist	47	74	7	–	0.020	<0.0001
Digoxin	14	33	2	–	0.067	0.028
Statin	42	21	46	–	0.054	0.83
Metformin	17	14	3	–	0.76	0.049
Bronchodilators	17	19	9	–	1.00	0.34
Hemodynamics						
HR, beats/min	75 ± 2	82 ± 4	74 ± 2	80 ± 16	0.073	0.71
LVPSP, mm Hg	166 ± 6	120 ± 3	223 ± 4	135 ± 15	<0.0001	<0.0001
LVEDP, mm Hg	25.1 ± 1.1	22.3 ± 1.4	22.8 ± 1.4	13 ± 4	0.12	0.21
LVEDVI, ml/m^2	80 ± 3	127 ± 5	55 ± 2	78 ± 23	<0.0001	<0.0001
% of LVEF	58.4 ± 2.1	29.4 ± 1.5	64.0 ± 1.2	73 ± 3	<0.0001	0.016

Values are mean ± SD or%.

ACEI = angiotensin-converting enzyme inhibitor; ARB = angiotensin II receptor blocker; AS = aortic stenosis; BMI = body mass index; DM = diabetes mellitus; HFpEF = heart failure with preserved ejection fraction; HFrEF indicates heart failure with reduced ejection fraction; HR = heart rate; LVEDP = left ventricular end-diastolic pressure; LVEDVI = left ventricular end-diastolic volume index; LVEF = left ventricular ejection fraction; LVPSP = left ventricular peak-systolic pressure.

Rat samples

Obese ZSF1 rats were previously shown to develop a HFpEF phenotype over a 20 weeks lifespan (15) and are referred to as ZSF1-HFpEF (N=8) in the present study. These rats are hypertensive and develop obesity and diabetes mellitus (DM) because of leptin resistance. ZSF1-lean rats are hypertensive, but do not develop obesity or DM and have no HFpEF phenotype (15). The ZSF1-lean rats are referred to as ZSF1-Ctrls (N=8) in the present study. All rats were sacrificed at 20 weeks of age.

Western blotting

Expression of total and phospho-proteins was measured in homogenized samples. The number of samples analysed was: ICAM-1: ZSF1-Ctrls:n=16, ZSF1-HFpEF:n=16, AS:n=4, HFrEF:n=7, HFpEF:n=4; E-selectin: AS:n=6, HFrEF:n=8, HFpEF:n=8; eNOS: ZSF1-Ctrls:n=8, ZSF1-HFpEF:n=8, AS:n=5, HFrEF:n=7, HFpEF:n=7; Kinases: ZSF1-Ctrls:n=8-10, ZSF1-HFpEF:n=8-10.

Immunofluorescence

Myocardial ICAM-1 expression was measured by immunofluorescence in frozen sections of 10µm thick rat myocardium: ZSF1-HFpEF:n=12, ZSF1-Ctrl:n=12.

Immunohistochemistry

For immunohistochemical staining of myeloperoxidase (MPO), CD68 and NADPH oxidase-2 (NOX2), paraffin embedded myocardial samples were used: MPO and CD68: ZSF1-Ctrl:n=8, ZSF1-HFpEF:n=8; NOX2: ZSF1-Ctrl:n=8, ZSF1-HFpEF:n=8, HFpEF:n=4, Ctrl patients:n=4.

Myocardial hydrogen peroxide quantification

Hydrogen peroxide (H_2O_2) was assessed in human and rat myocardial tissue homogenates (ZSF1-Ctrl:n=10; ZSF1-HFpEF:n=10, AS:n=16, HFrEF:n=16, HFpEF:n=16.

Nitrate/nitrite concentration

The concentrations of nitrite/nitrate were measured in tissue homogenates (ZSF1-Ctrl:n=10, ZSF1-HFPEF:n=10, AS:n=16, HFpEF:n=16, HFrEF:n=16) by means of a colorimetric assay kit (BioVision).

Immunoelectron microscopic quantification of 3-nitrotyrosine

A standard pre-embedding immunogold electron microscopy protocol was used to quantify myocardial 3-nitrotyrosine in rats (ZSF1-HFpEF:n=6, ZSF1-Ctrl:n=6).

Myocardial PKA, PKC, PKG, cGMP and CaMKII activity

Kinase activities were assessed in myocardial homogenates. Activities (ZSF1-HFpEF:n=10, ZSF1-Ctrl:n=10) were analyzed as described previously for PKA and PKC (17) and for PKG and cGMP (18).

CaMKII activity was determined using a CycLex® CaMKII assay kit (ZSF1-HFpEF:n=10, ZSF1-Ctrl:n=10).

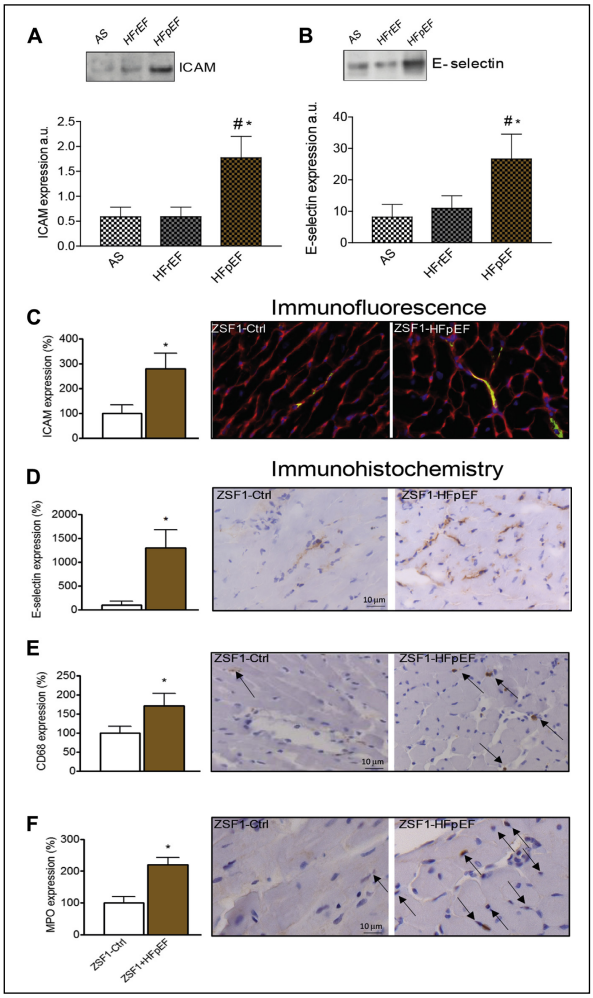

Figure 1. (**A**) ICAM-1 expression was higher in HFpEF than in AS (#p < 0.05 vs. AS;*p < 0.05 vs. HFrEF). (**B**) E-selectin levels were higher in HFpEF patients than in those with HFrEF and AS (#p < 0.05 vs. AS; *p < 0.05 vs. HFrEF). Expression levels of ICAM-1 (**C**) and E-selectin (**D**) were higher in ZSF1-HFpEF myocardium than in that of ZSF1-Ctrls (*p < 0.05). (E and F) ZSF1-HFpEF rats had higher levels of myocardial CD68 and MPO than ZSF1-Ctrls (*p < 0.05). AS = aortic stenosis; Ctrls = controls; HFpEF = heart failure with preserved ejection fraction; HFrEF = heart failure with reduced ejection fraction; ICAM = intercellular adhesion molecule; MPO = myeloperoxidase.

Statistical analysis

Differences between groups were analyzed by one-way ANOVA followed by Bonferroni-adjusted t tests. Single comparisons were assessed by an unpaired Student t test. All analyses were performed using Prism software (GraphPad Software Inc, version 6.0).

RESULTS

Patient characteristics

More HFpEF than HFrEF patients were hypertensive and DM was more prevalent in HFpEF compared to AS (see Table). Body mass index (BMI) was higher in HFpEF

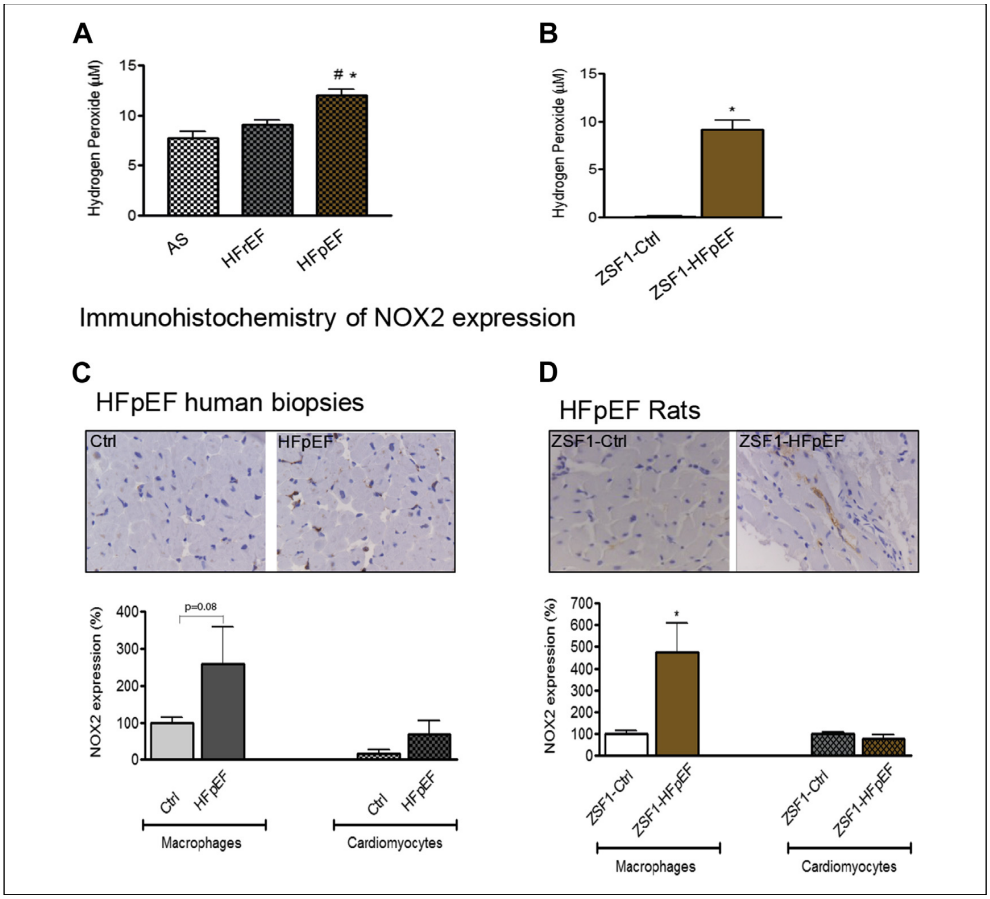

Figure 2. (**A**) HFpEF patients had higher myocardial concentrations of H_2O_2 than AS and HFrEF (#p < 0.05 vs. AS; *p < 0.05 vs. HFrEF). (**B**) Myocardial H_2O_2 concentrations in ZSF1-HFpEF were higher than in ZSF1-Ctrl rats (*p < 0.05). (**C**) Expression of NOX2 was comparable in cardiomyocytes but tended to be higher in macrophages of HFpEF patients. (**D**) Expression of NOX2 was comparable in cardiomyocytes of ZSF1-Ctrl and ZSF1- HFpEF rats. More NOX2-expressing macrophages were observed in ZSF1-HFpEF rats (*p < 0.05 vs. controls). NOX2 = NADPH oxidase 2; other abbreviations as in Figure 1.

versus AS patients. Angiotensin converting enzyme inhibitors or angiotensin II receptor blockers, diuretics and digoxin were more frequently used in HFpEF and HFrEF compared to AS patients. Aldosterone receptor antagonists were used more in HFpEF than in AS, but even more in HFrEF patients. LV peak systolic pressure and LVEF were higher in HFpEF than in HFrEF but highest in AS patients. LV end diastolic volume index was lower in HFpEF than in HFrEF but the lowest in AS patients. LV end diastolic pressures were equally elevated in all patient groups.

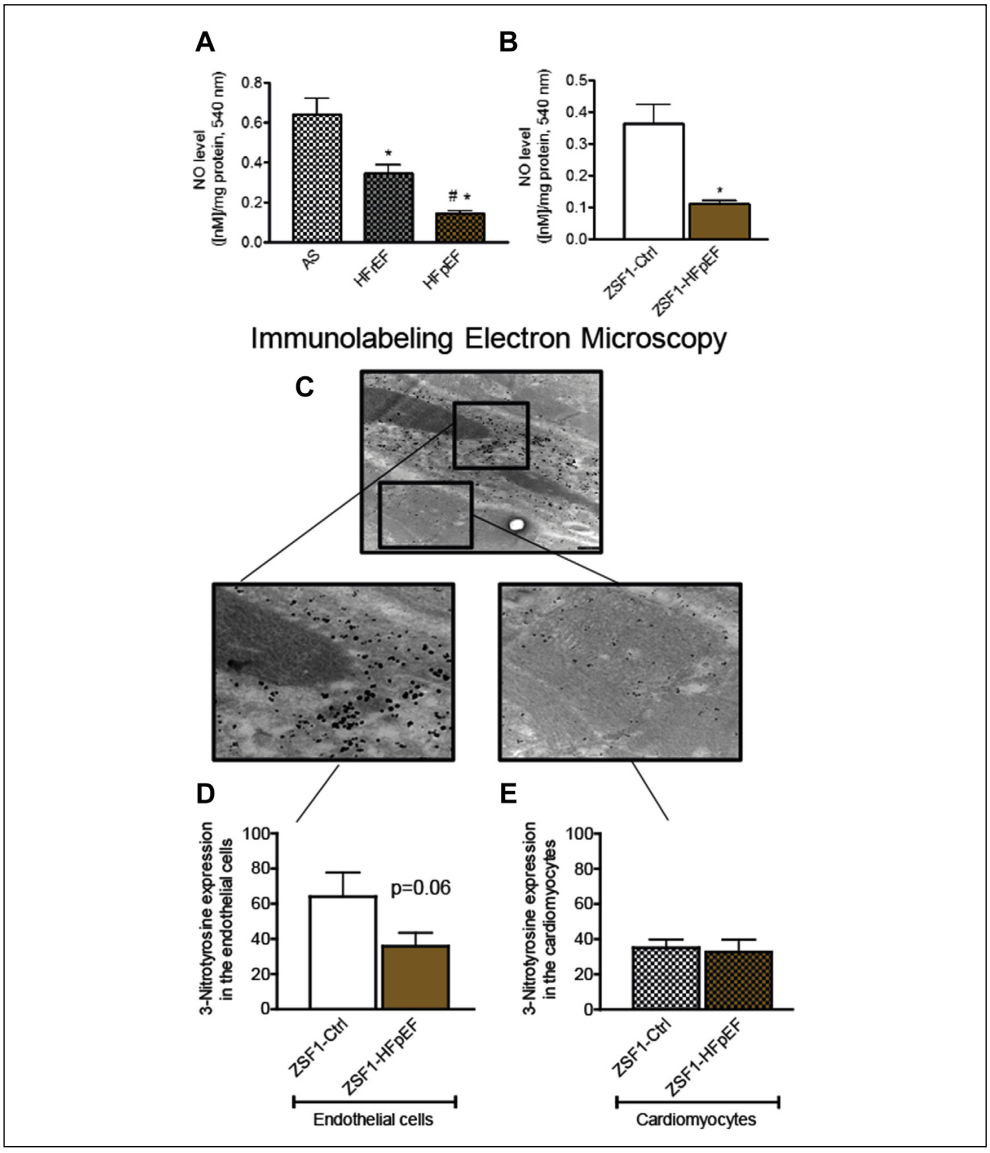

Figure 3. (**A**) Myocardial nitrite/nitrate concentrations were lower in HFpEF than in AS and HFrEF patients and lower in HFrEF than in AS patients (*p < 0.05 HFpEF vs. AS; #p < 0.05, HFpEF vs. HFrEF; *p < 0.05, HFrEF vs. AS). (**B**) Myocardial nitrite/nitrate concentrations were lower in ZSF1-HFpEF than in ZSF1-Ctrl rats (*p < 0.05 vs. controls). (**C**) Immunogold-labeled electron microscopy showed myocardial localization of 3-nitrotyrosine. (**D**) 3-Nitrotyrosine expression tended to decrease more in endothelial cells of ZSF1-HFpEF than those of ZSF1-Ctrl rats. (**E**) 3-Nitrotyrosine expression was similar in cardiomyocytes of ZSF1-HFpEF and ZSF1-Ctrl rats. NO = nitric oxide; other abbreviations as in Figure 1.

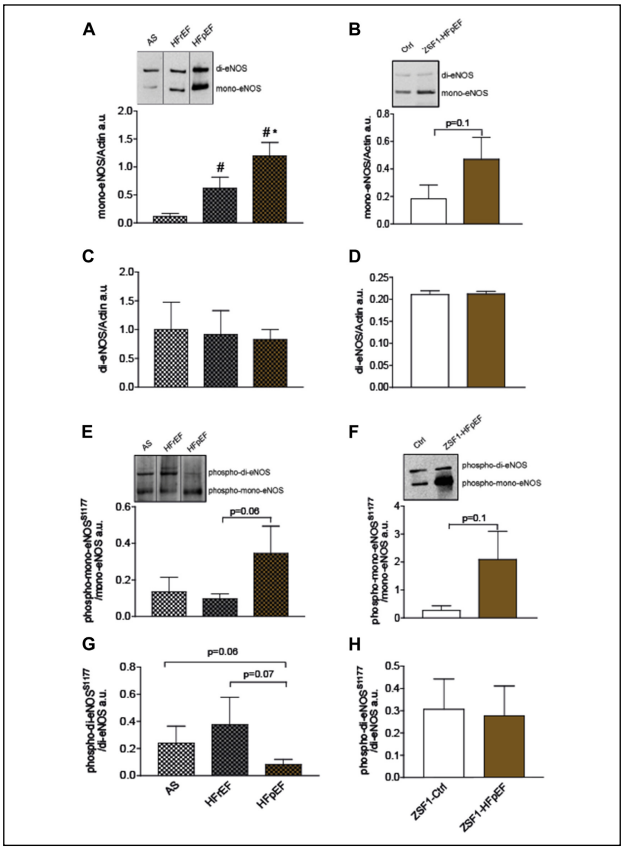

Figure 4. (**A**) Expression of eNOS monomer was higher in HFpEF than in AS and HFrEF and higher in HFrEF than in AS (#p < 0.05 vs. AS; *p < 0.05 vs. HFrEF). (**B**) A similar trend was observed in a comparison between ZSF1-HFpEF and ZSF1-Ctrl rats. (**C** and **D**) eNOS dimer concentrations were comparable in AS, HFrEF, and HFpEF patients as well as in ZSF1-HFpEF and ZSF1-Ctrl rats. (**E** and **F**) eNOS momomer phosphorylation tended to be higher in HFpEF patients and in ZSF1-HFpEF rats. (**G** and **H**) eNOS dimer phosphorylation tended to be lower in HFpEF patients but was comparable in rats. eNOS = endothelial nitric oxide synthase; other abbreviations as in Figure 1.

Microvascular inflammation and macrophage activation in HFpEF

Microvascular inflammation and macrophage activation were assessed by expression of the vascular adhesion molecules ICAM-1 and E-selectin. Both markers were increased in HFpEF compared to AS or HFrEF (Figure 1A-B), consistent with the comorbidities-induced pro-inflammatory status of HFpEF patients.

Similarly, immunofluorescence showed increased endothelial ICAM-1 and E-selectin expression in ZSF1-HFpEF rats compared to ZSF1-Ctrls (Figure 1C-D). ZSF1-HFpEF rats also had higher myocardial CD68 and MPO expression than ZSF1-Ctrl, indicating monocyte/macrophage recruitment and neutrophil activation (Figures 1E-F).

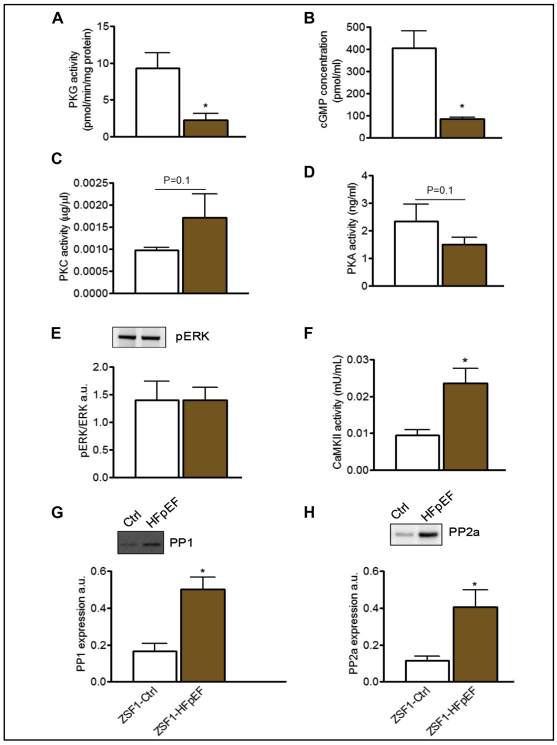

Figure 5. (**A** and **B**) Myocardial PKG activity and cGMP concentration were lower in ZSF1-HFpEF than in ZSF1-Ctrl rats. (**C** and **D**) Comparable activity levels of PKC and PKA were seen in ZSF1-HFpEF and ZSF1-Ctrl rats. (**E**) Comparable expression levels of phosphorylated ERK were seen in ZSF1-HFpEF and ZSF1-Ctrl rats. (**F**) Expression of CaMKII was higher in ZSF1-HFpEF than in ZSF1-Ctrl rats. (**G** and **H**) Higher expression of PP1 and PP2a was seen in ZSF1-HFpEF than in ZSF1-Ctrl rats (*p < 0.05). CaMKII = Ca^{2+}/calmodulin-dependent protein kinase II; cGMP = cyclic guanosine monophosphate; ERK = extracellular signal-regulated kinase; PKA = protein kinase A; PKC = protein kinase C; other abbreviations as in Figure 1.

Increased oxidative stress in HFpE

To quantify myocardial oxidative stress, H_2O_2 concentrations were shown to be higher in HFpEF than in HFrEF and AS patients (Figure 2A), again consistent with the comorbidities-induced pro-inflammatory status of the HFpEF patients. Findings were reproduced in ZSF1-HFpEF rats which also had increased myocardial H_2O_2 levels compared to ZSF1-Ctrl (Figure 2B).

To account for the myocardial oxidative stress, expression of NOX2 was compared between HFpEF patients and controls. Human HFpEF myocardium contained more NOX2 expressing macrophages than control (Figure 2C). Expression in cardiomyocytes was however comparable in both HFpEF patients and controls (Figure 2C). Findings were confirmed in ZSF1-HFpEF myocardium by the presence of more NOX2 expressing macrophages than in ZSF1-Ctrl. Similar to the human findings, NOX2 expression was equal in cardiomyocytes of ZSF1-HFpEF and ZSF1-Ctrl rats (Figure 2D). Furthermore, NOX2 expression was also manifest in microvascular endothelial cells of ZSF1-HFpEF rats (Figure 2D), indicative of a systemic pro-inflammatory status.

Decreased NO bioavailability in HFpEF

Because of the high oxidative stress, bioavailability of NO gets jeopardized. NO bioavailability was therefore assessed by measurement of myocardial nitrite/ nitrate concentrations in human biopsies. Nitrite/nitrate concentration was indeed lower in HFpEF than in AS and HFrEF (Figure 3A). These findings were also confirmed in the rat model (Figure 3B).

Furthermore, immunogold labeled electron microscopy allowed for quantification of 3-nitrotyrosine in different myocardial cellular compartments (Figure 3C). 3-Nitrotyrosine formation reflects concentration of peroxynitrite, which is generated from superoxide anion and NO. 3-Nitrotyrosine expression was higher in endothelial cells compared to cardiomyocytes (Figure 3D-E). Its endothelial expression tended to decrease in ZSF1-HFpEF (Figure 3D) probably as a result of reduced NO bioavailability, whereas cardiomyocyte expression remained unaltered (Figure 3E).

Uncoupling of nitric oxide synthase in HFpEF

Endothelial nitric oxide synthase (eNOS) produces NO as a dimer, but "uncouples" into monomers in the presence of inflammation/oxidative stress, producing superoxide anion. HFpEF patients had significantly higher expression of the eNOS monomer than HFrEF or AS patients (Figure 4A). In ZSF1-HFpEF rats, there was a similar trend for higher expression of the eNOS monomer compared to ZSF1-Ctrl (Figure 4B). Levels of eNOS dimers were equal among human groups and between the two groups of rats (Figures 4C-D). Phosphorylated and hence activated eNOS monomers tended to be higher in HFpEF compared to HFrEF and AS patients (P=0.06) and in ZSF1-HFpEF compared to ZSF1-Ctrl rats (Figures 4E-F). The concentration of active, phosphorylated NO-producing dimer was lower in HFpEF compared to AS (P=0.06) and HFrEF (P=0.07) patients (Figure 4G). In rats, phosphorylation of the eNOS dimer was similar (Figure 4H).

Decreased cGMP concentration and PKG activity in HFpEF

Because of decreased NO bioavailability, soluble guanylate cyclase (sGC) activity falls. This leads to reduced production of cGMP, which regulates PKG activity. PKG acitivity and cGMP concentration were indeed lower in myocardium of ZSF1-HFpEF rats compared to ZSF1-Ctrl (Figure 5A-B).. PKG lowers cardiomyocyte stiffness through phosphorylation of titin, the giant intracellular protein responsible for cardiomyocyte based stiffness (15, 17–19). Activity and expression

of other protein kinases and phosphatases, reported to modulate titin phosphorylation (19) were measured as well. Activities of protein kinase C (PKC) and A (PKA) were not significantly different between ZSF1-HFpEF and ZSF1- Ctrl rats (Figures 5C-D). There was no significant difference in expression of the active, phosphorylated state of extracellular-signal-regulated kinase (ERK) between ZSF1-HFpEF rats and Ctrl rats (Figure 5E). Ca^{2+}/calmodulin-dependent protein kinase-II (CaMKII) also lowers cardiomyocyte stiffness through titin phosphorylation (20). CaMKII activity was increased in ZSF1-HFpEF rats compared to ZSF1-Ctrl rats (Figure 5F) and altered CaMKII activity therefore fails to explain the increased cardiomyocyte stiffness observed in previous experiments in ZSF1-HFpEF rats (15). Finally, titin can also be affected by dephosphorylating protein phosphatases (PP) such as PP1 and PP2a (19). Both were increased in ZSF1-HFpEF compared to ZSF1-Ctrl rats (Figures 5G-H).

DISCUSSION

The present study provides comprehensive evidence for microvascular endothelial activation, high oxidative stress, eNOS-uncoupling and low NO level in LV myocardium of HFpEF patients. These findings were reproduced in leptin-resistant, obese hypertensive ZSF1 rats, which develop HFpEF after 20 weeks in contrast to lean hypertensive ZSF1 rats, which maintain normal LV function after a similar time period. The present study also demonstrated that the low myocardial NO level was associated with reduced myocardial cGMP/PKG signalling in ZSF1-HFPEF rats. A similar reduction was previously demonstrated in LV myocardium of HFpEF patients and shown to be associated with titin hypophosphorylation which contributes to high myocardial diastolic stiffness (18).

Microvascular inflammation

In the present study, myocardial expression of E-selectin and ICAM-1 was upregulated in HFpEF patients and ZSF1-HFpEF rats (Figure 6). Upregulated myocardial expression of Vascular Cell Adhesion Molecule (VCAM) and myocardial microvascular rarefaction compatible with microvascular inflammation had previously already been reported in HFpEF (22,23). Because of the similarity of findings in HFpEF patients and ZSF1-HFpEF rats, we attribute the endothelial inflammatory activation in HFpEF patients to their metabolic risk profile. HFpEF

patients had significantly higher BMI than AS and HFrEF patients and the prevalence of DM was also higher in the HFpEF than in AS patients. The high prevalence of a metabolic risk profile in HFpEF patients of the present study was consistent with the findings of the recent MEDIA European HFpEF registry (23). This registry was the first to report on the prevalence of metabolic syndrome in HFpEF and observed 85% of HFpEF patients to satisfy the National Cholesterol Education Program III criteria of metabolic syndrome.

Expression of adhesion molecules favours myocardial infiltration of inflammatory cells, which was evident in the current study in HFpEF patients and in ZSF1-HFpEF rats respectively by the presence of NOX2 producing macrophages and by the high expression of CD68 and MPO. In contrast to viral myocarditis, the myocardial presence in HFpEF of macrophages is not accompanied by evidence of cardiomyocyte cell death (25,26). A recent study provides an explanation for this intriguing finding as it observed macrophages activated by obesity to have a distinct proinflammatory phenotype (26). Hitherto macrophage activation was conceived to proceed either to a M1 phenotype with potent proinflammatory properties or to a M2 phenotype with anti-inflammatory properties. However, when macrophages are activated by obesity, a distinct phenotype is induced with low production of proinflammatory cytokines because of peroxisome proliferator-activated receptor ɣ (PPAR ɣ) partially inhibiting induction of nuclear factor kappa-light-chain-enhancer of activated B cells (NFκB). This last effect results from the abundance in obesity of free fatty acids such as palmitate, which stimulate PPAR ɣ activity. A recent study also demonstrated HFpEF development to be associated with monocytosis and monocyte differentiation into M2-macrophages (27).

Oxidative stress

Myocardial H_2O_2 concentration was significantly higher in HFpEF than in both HFrEF and AS. Similarly, ZSF1-HFpEF rats had higher myocardial H_2O_2 concentrations than ZSF1-Ctrl animals. H_2O_2 results from conversion of superoxide anion by superoxide dismutase and the high H_2O_2 concentrations therefore suggest increased superoxide anion production in HFpEF. Possible sources of superoxide anion production are NADPH oxidases (NOX2, NOX4), uncoupled NO synthases (eNOS, iNOS), xanthine oxidase and mitochondria (Figure 6). The cellular localization of NOX2 expression was immunohistochemically visualized in myocardial tissue of HFpEF patients and ZSF1-HFpEF rats. Upregulation of NOX2 expression was observed in macrophages and microvascular endothelium but not

in cardiomyocytes. The current findings of upregulated endothelial NOX2 expression and unaltered NOX2 expression in cardiomyocytes in HFpEF myocardium support myocardial remodeling in HFpEF to be driven by endothelial activation in contrast to HFrEF, where myocardial remodeling is driven by cardiomyocyte cell death triggered by upregulated NOX2 activity within cardiomyocytes (28).

NO-cGMP-PKG signalling

Similar to NOX2 expression, immunoelectron microscopy revealed myocardial 3-nitrotyrosine expression in ZSF1-Ctrl and ZSF1-HFpEF rats to be mainly localized in endothelial cells with less expression in cardiomyocytes. HFpEF development failed to affect 3-nitrotyrosine expression in cardiomyocytes but reduced 3-nitrotyrosine expression in endothelial cells. 3-Nitrotyrosine formation reflects peroxynitrite concentration, which is generated from superoxide anion and NO. Because of increased H_2O_2 concentration, the trend for reduced 3-nitrotyrosine in endothelial cells of HFpEF myocardium probably resulted from low NO production. The latter was consistent with the low nitrite/nitrate concentrations observed in myocardium of both HFpEF patients and ZSF1-HFpEF rats. Reduced NO production can be explained by eNOS uncoupling, which was confirmed in both HFpEF patients and ZSF1-HFpEF rats. eNOS uncoupling switches eNOS from the NO producing dimer to the superoxide anion generating monomer (29). Apart from eNOS uncoupling, the present study also observed modified eNOS phosphorylation in HFpEF patients with a higher phosphorylation of monomeric eNOS increasing superoxide production and a lower phosphorylation of dimeric eNOS decreasing NO production. Low NO production affects sGC activity and results in decreased levels of cGMP and low PKG activity (Figure 6). This was previously observed in human HFpEF myocardium (18) and currently confirmed in ZSF1-HFpEF myocardium. Low PKG activity increases diastolic stiffness through reduced phosphorylation of the giant cytoskeletal protein titin (Figure 6) (31,32).

The phosphorylation and distensibility of titin are also affected by phosphatases and other kinases, such as PKC, PKA, ERK and CaMKII (20,31,32). In the present study, ZSF1-HFpEF rats showed higher expression of PP1 and PP2a. PKC, PKA and ERK activities were comparable but CaMKII activity was increased. Phosphorylation of titin by CaMKII augments titin distensibility (32) and the higher CaMKII activity therefore cannot explain the high cardiomyocyte resting tension

previously observed in ZSF1-HFpEF rats (15). The latter more likely results from imbalanced activities of PKG and phosphatases.

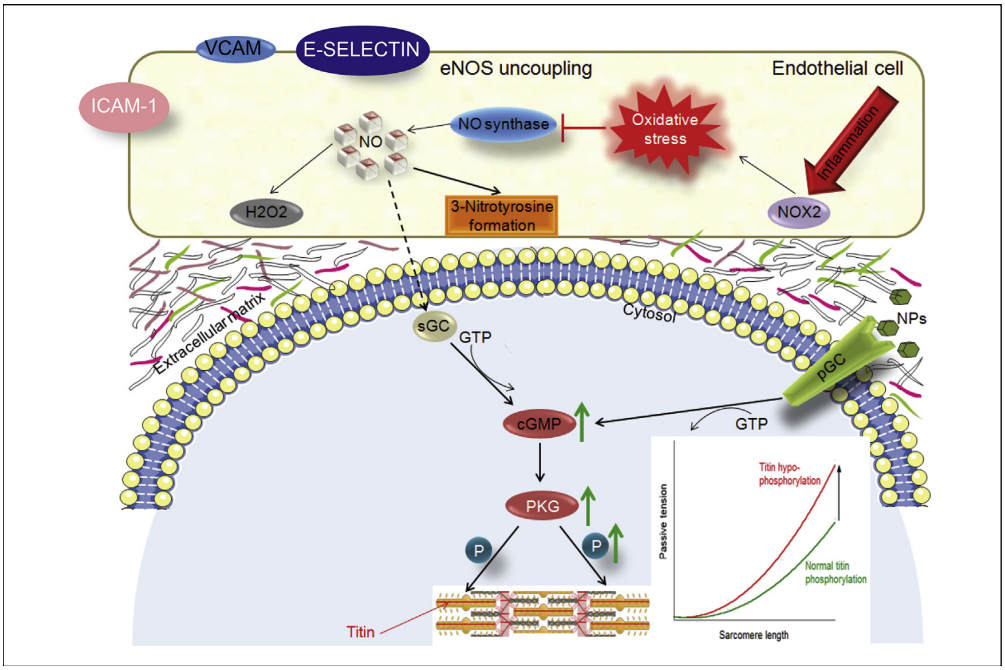

Figure 6. Systemic inflammation induces inflammatory activation of the endothelium of myocardial microcirculation. This leads to enhanced endothelial expression of adhesion molecules such as ICAM-1, VCAM, and E-selectin. Because of inflammatory activation, NOX2 is upregulated in endo- thelial cells. This results in oxidative stress, increased levels of H_2O_2, uncoupling of eNOS, decreased NO bioavailability, and formation of 3-nitrotyrosine. In cardiomyocytes, decreased NO bioavailability leads to less stimulation of sGC, reduced formation of cGMP, and diminished PKG activity. Lack of PKG activity is associated with decreased titin phosphorylation and increased passive stiffness of cardiomyocytes. cGMP can also be generated by NPs which activate pGC. Because of the low cGMP concentration, the latter pathway failed to compensate for the decreased NO-bioavailability. cGMP = cyclic guanosine monophosphate; eNOS = endothelial nitric oxide synthase; H_2O_2 = hydrogen peroxide; ICAM-1 = intercellular adhesion molecule-1; NO = nitric oxide; NOX2 = NADPH nicotinamide adenine dinucleotide phosphate oxidase 2; NPs = natriuretic peptides; pGC = particulate guanylate cyclase; PKG = protein kinase G; sGC = soluble guanylate cyclase; VCAM = vascular cell adhesion molecule.

LIMITATIONS

Except for immunohistochemical assessment of NOX2 expression, the present study compares myocardial tissue of HFpEF patients to tissue of HFrEF and AS patients because of limited availability of myocardial tissue from control subjects. This limitation was partially accounted for by inclusion of an animal model consisting of obese and lean ZSF1 rats (15). Both HFpEF and HFrEF patients were investigated following an acute heart failure admission. An inflammatory component related to the acute heart failure episode could have contributed to the microvascular inflammation.

CONCLUSIONS

Microvascular inflammatory endothelial activation, high oxidative stress, eNOS uncoupling and impaired cGMP-PKG signalling were observed in LV myocardium of HFpEF patients. Similar changes were reproduced in obese, leptin-resistant, hypertensive ZSF1 rats, which developed a HFpEF phenotype after 20 weeks, but not in lean, hypertensive ZSF1 rats. Because of these findings, myocardial microvascular inflammation induced by metabolic comorbidities could be an important contributor to HFpEF development.

PERSPECTIVES

Clinical competencies - Metabolic comorbidities such as obesity and DM induce chronic endothelial inflammation of the coronary microvasculature, which reduces myocardial NO bioavailability, PKG activity and cGMP concentration. The latter predisposes to cardiomyocyte stiffness and hypertrophy, both of which are characteristic for HFpEF.

Translational outlook – Future therapeutic strategies in HFPEF should target the metabolic risk-induced chronic inflammation of the myocardial microvasculature.

REFERENCES

1. Borlaug BA, Redfield MM, Melenovsky V, et al. Longitudinal changes in left ventricular stiffness: a community-based study. Circ. Heart Fail. 2013;6:944–52.

2. Wohlfahrt P, Redfield MM, Lopez-Jimenez F, et al. Impact of general and central adiposity on ventricular-arterial aging in women and men. JACC. Heart Fail. 2014;2:489–99.

3. Davis BR, Kostis JB, Simpson LM, et al. Heart failure with preserved and reduced left ventricular ejection fraction in the antihypertensive and lipid-lowering treatment to prevent heart attack trial. Circulation 2008;118:2259–67.

4. Chadderdon SM, Belcik JT, Bader L, et al. Proinflammatory endothelial activation detected by molecular imaging in obese nonhuman primates coincides with onset of insulin resistance and progressively increases with duration of insulin resistance. Circulation 2014;129:471–8.

5. Katz DH, Selvaraj S, Aguilar FG, et al. Association of low-grade albuminuria with adverse cardiac mechanics: findings from the hypertension genetic epidemiology network (HyperGEN) study. Circulation 2014;129:42–50.

6. Brouwers FP, de Boer RA, van der Harst P, et al. Incidence and epidemiology of new onset heart failure with preserved vs. reduced ejection fraction in a community-based cohort: 11-year follow-up of PREVEND. Eur. Heart J. 2013;34:1424–31.

7. Bonetti PO, Pumper GM, Higano ST, Holmes DR, Kuvin JT, Lerman A. Noninvasive identification of patients with early coronary atherosclerosis by assessment of digital reactive hyperemia. J. Am. Coll. Cardiol. 2004;44:2137–2141.

8. Akiyama E, Sugiyama S, Matsuzawa Y, et al. Incremental prognostic significance of peripheral endothelial dysfunction in patients with heart failure with normal left ventricular ejection fraction. J. Am. Coll. Cardiol. 2012;60:1778–86.

9. Lam CSP, Brutsaert DL. Endothelial dysfunction: a pathophysiologic factor in heart failure with preserved ejection fraction. J. Am. Coll. Cardiol. 2012;60:1787–9.

10. Borlaug BA, Olson TP, Lam CSP, et al. Global cardiovascular reserve dysfunction in heart failure with preserved ejection fraction. J. Am. Coll. Cardiol. 2010;56:845–54.

11. Farrero M, Blanco I, Batlle M, et al. Pulmonary hypertension is related to peripheral endothelial dysfunction in heart failure with preserved ejection fraction. Circ. Heart Fail. 2014;7:791–8.

12. Paulus WJ, Tschöpe C. A novel paradigm for heart failure with preserved ejection fraction: comorbidities drive myocardial dysfunction and remodeling through coronary microvascular endothelial inflammation. J. Am. Coll. Cardiol. 2013;62:263–71.

13. González A, Ravassa S, Beaumont J, López B, Díez J. New targets to treat the structural remodeling of the myocardium. J. Am. Coll. Cardiol. 2011;58:1833–43.

14. Grossman W, Paulus WJ. Myocardial stress and hypertrophy: a complex interface between biophysics and cardiac remodeling. J. Clin. Invest. 2013;123:3701–3.

15. Hamdani N, Franssen C, Lourenço A, et al. Myocardial titin hypophosphorylation importantly contributes to heart failure with preserved ejection fraction in a rat metabolic risk model. Circ. Heart Fail. 2013;6:1239–49.

16. Paulus WJ, Tschöpe C, Sanderson JE, et al. How to diagnose diastolic heart failure: a consensus statement on the diagnosis of heart failure with normal left ventricular ejection fraction by the Heart Failure and Echocardiography Associations of the European Society of Cardiology. Eur. Heart J. 2007;28:2539–50.

17. Hamdani N, Bishu KG, von Frieling-Salewsky M, Redfield MM, Linke WA. Deranged myofilament phosphorylation and function in experimental heart failure with preserved ejection fraction. Cardiovasc. Res. 2013;97:464–71.

18. Van Heerebeek L, Hamdani N, Falcão-Pires I, et al. Low myocardial protein kinase g activity in heart failure with preserved ejection fraction. Circulation 2012;126:830–9.

19. Linke WA, Hamdani N. Gigantic business: titin properties and function through thick and thin. Circ. Res. 2014;114:1052–68.

20. Hidalgo CG, Chung CS, Saripalli C, et al. The multifunctional Ca(2+)/calmodulin-dependent protein kinase II delta (CaMKIIδ) phosphorylates cardiac titin's spring elements. J. Mol. Cell. Cardiol. 2013;54:90–7.

21. Westermann D, Lindner D, Kasner M, et al. Cardiac inflammation contributes to changes in the extracellular matrix in patients with heart failure and normal ejection fraction. Circ. Heart Fail. 2011;4:44–52.

22. Mohammed SF, Hussain S, Mirzoyev SA, et al. Coronary Microvascular Rarefaction and Myocardial Fibrosis in Heart Failure With Preserved Ejection Fraction. Circulation 2014;131:550–559.

23. Dobre D, Girerd N, Rossignol P, et al. Comparison of the echocardiographic definition of left ventricular diastolic dysfunction using the 2007 ESC and the 2009 EAE/ASE recommendations in metabolic syndrome patients. In: European Heart Journal., 2014:35 (Abstract Supplement), 1037.

24. Van Heerebeek L, Borbély A, Niessen HWM, et al. Myocardial structure and function differ in systolic and diastolic heart failure. Circulation 2006;113:1966–73.

25. Van Heerebeek L, Hamdani N, Handoko ML, et al. Diastolic stiffness of the failing diabetic heart: importance of fibrosis, advanced glycation end products, and myocyte resting tension. Circulation 2008;117:43–51.

26. Kratz M, Coats BR, Hisert KB, et al. Metabolic dysfunction drives a mechanistically distinct proinflammatory phenotype in adipose tissue macrophages. Cell Metab. 2014;20:614–25.

27. Glezeva N, Voon V, Watson C, et al. Exaggerated inflammation and monocytosis associate with diastolic dysfunction in heart failure with preserved ejection fraction: evidence of M2 macrophage activation in disease pathogenesis. J. Card. Fail. 2015;21:167–77.

28. Zhang M, Perino A, Ghigo A, Hirsch E, Shah AM. NADPH oxidases in heart failure: poachers or gamekeepers? Antioxid. Redox Signal. 2013;18:1024–41.

29. Silberman GA, Fan T-HM, Liu H, et al. Uncoupled cardiac nitric oxide synthase mediates diastolic dysfunction. Circulation 2010;121:519–28.

30. Krüger M, Kötter S, Grützner A, et al. Protein kinase G modulates human myocardial passive stiffness by phosphorylation of the titin springs. Circ. Res. 2009;104:87–94.

31. Zile MR, Baicu CF, Ikonomidis J, et al. Myocardial Stiffness in Patients with Heart Failure and a Preserved Ejection Fraction: Contributions of Collagen and Titin. Circulation 2015;131:1247–59.

32. Hamdani N, Krysiak J, Kreusser MM, et al. Crucial role for Ca2(+)/calmodulin-dependent protein kinase-II in regulating diastolic stress of normal and failing hearts via titin phosphorylation. Circ. Res. 2013;112:664–74.

ONLINE DATA SUPPLEMENT: METHOD SECTION

METHODS

Human samples

Human HFrEF and HFpEF samples were procured from LV biopsies [HFrEF (N=43) and HFpEF (N=36)]. HFrEF and HFpEF patients were hospitalized for HF and underwent transvascular LV endomyocardial biopsy procurement because of suspicion of an infiltrative or inflammatory cardiomyopathy. Patients were included if significant coronary artery disease (stenosis >50%) was ruled out by angiography and if histological analysis of the biopsy showed no evidence of infiltrative or inflammatory myocardial disease. Patients were classified as HFpEF if LVEF was >50%, LV end diastolic volume index <97 ml/m^2, and LV end-diastolic pressure was >16 mmHg (16). If LVEF was <45%, a patient was classified as HFrEF. AS patients (N=67) had severe AS (mean aortic valve area 0.53±0.04cm^2) without concomitant coronary artery disease. Biopsy specimens from this group were procured from endomyocardial tissue resected from the septum (Morrow procedure) during aortic valve replacement. The local ethics committee approved the study protocol. Written informed consent was obtained from all patients. Control human samples (N=4) were procured from patients with life-threatening arrhythmias, suspected infiltrative heart disease or myocarditis and a preserved LVEF without coronary artery disease in whom histology ruled out myocarditis or infiltrative pathology. Because of limited availability of human myocardial tissue, histological and biochemical determinations could only be performed in subgroups of patients, randomly selected by blinded investigators.

Rat samples

Obese ZSF1 rats were previously shown to develop a HFpEF phenotype over a 20 weeks lifespan (15) and are referred to as ZSF1-HFpEF (N=8) in the present study. These rats are hypertensive and develop obesity and diabetes mellitus (DM) because of leptin resistance. ZSF1-lean rats are hypertensive, but do not develop obesity or DM and have no HFpEF phenotype (15). The ZSF1-lean rats are referred to as ZSF1-Ctrls (N=8) in the present study. All rats were sacrificed at 20 weeks of age.

Western blotting

Expression of total and phospho-proteins was measured by 15% SDS-PAGE and Western blot in homogenized samples. Hybond ECL nitrocellulose membranes (GE Healthcare) were used in combination with the following primary rabbit or mouse polyclonal antibodies: against eNOS and phospho-eNOS (1:1000, Abcam), Intercellular Adhesion Molecule 1 (ICAM-1, 1:200, Abcam), E-selectin (1:250, Abcam), ERK (1:1000, Cell Signalling), phospho-ERK (1:1000, Cell Signalling), PP1 (1:200, Santa Cruz Biotechnology) and PP2a (1:500, Upstate). All signals were normalized to β-actin peroxidase antibody (dilution 1:1000; clone KJ43A; Sigma). Staining was visualized using the LAS-3000 Image Reader (460nm/605nm Ex/Em; 2s illumination) and signals were analyzed with AIDA software. The number of samples analysed was: ICAM-1: ZSF1-Ctrls:n=16, ZSF1-HFpEF: n=16, AS:n=4, HFrEF:n=7, HFpEF:n=4; E-selectin: AS:n=6, HFrEF:n=8, HFpEF:n=8; eNOS: ZSF1-Ctrls:n=8, ZSF1-HFpEF:n=8, AS:n=5, HFrEF:n=7, HFpEF:n=7; Kinases: ZSF1-HFpEF:n=8-10, ZSF1-Ctrls:n=8-10.

Immunofluorescence

Myocardial ICAM-1 expression was measured by immunofluorescence in rats. Frozen sections of 10µm thick rat myocardium (ZSF1-HFpEF:n=12, ZSF1-Ctrl:n=12;) were fixated in 4% paraformaldehyde and washed in 0.05% PBS-Tween. Tissue sections were incubated with primary antibody against ICAM-1 at 4°C (1:100, Abcam). After rinsing with PBS-Tween, sections were incubated with secondary antibody donkey anti-mouse Alexafluor-488 (1:1000, Invitrogen). After washing in PBS-Tween samples were incubated with Wheat Germ Agglutination Conjugate Alexafluor-555 (WGA, 1:1000, Invitrogen). After rinsing again in PBS-Tween and PBS, coverslips were mounted onto the glass slides using mounting medium with DAPI (Vectashield). Images were acquired with a fluorescence microscope and quantified in Slidebook (3i). ICAM-1 staining was displayed with FITC and sum intensities were acquired. The results were expressed as a percentage of the control (set at 100%).

Immunohistochemistry

For immunohistochemical staining of myeloperoxidase (MPO), CD68 and NADPH oxidase-2 (NOX2), paraffin embedded myocardial samples (MPO and CD68: ZSF1-HFpEF:n=8, ZSF1-Ctrl:n=8; NOX2: ZSF1-HFpEF: n=8, ZSF1-Ctrl:n=8; HFpEF: n=4, Ctrl patients:n=4) were dewaxed and rehydrated in xylene and alcohol (100%)

followed by incubation in 0,3% methanol/H_2O_2 to block endogenous peroxidases. Antigen retrieval was performed by either boiling slides in a citrate pH 6.0 (MPO) or a Tris-EDTA pH 9.0 (NOX2) solution or by incubation with 0,1% pepsin/HCl (CD68). Next, sections were incubated with rabbit anti-rat MPO (1:50, Abcam), mouse anti-rat CD68 (1:400, Serotec), or mouse anti-NOX2 (1:10, CLB). Sections were then incubated with undiluted goat anti-mouse/rabbit envision (Dako).

For immunohistochemical staining of E-selectin (CD62e), frozen myocardial tissues (ZSF1-HFpEF:n=8, ZSF1-Ctrl:n=8;) were fixated in followed by incubation in 0,3% methanol/H_2O_2 to block endogenous peroxidases. Next, sections were pre-incubated with 1:500 normal rabbit serum (Dako), followed by incubation with goat anti-rat CD62e (1:100, LifeSpan BioSciences) primary antibody. Sections were then incubated with rabbit anti-goat-HRP (1:100, Dako). Staining for all markers was visualized using 3,3'-diaminobenzidine (0.1mg/mL, 0.02% H2O2), and sections were counterstained with haematoxylin, dehydrated, and covered. Negative and positive controls were performed in parallel to all staining series.

Light microscopy (Olympus BX50) was used for the quantitative analysis. Macrophages and cardiomyocytes were manually counted. Analysis of tissue areas was performed using Slidebook (3i). The staining density was calculated as the number of stained macrophages or cardiomyocyte nuclei per unit area of myocardium. These results are expressed as a percentage of the control (set at 100%).

Myocardial hydrogen peroxide quantification

Hydrogen peroxide (H_2O_2) was assessed in human and rat myocardial tissue homogenates (ZSF1-HFpEF:n=10, ZSF1-Ctrl:n=10; AS:n=16, HFrEF:n=16, HFpEF: n=16). Samples containing equal amounts of total protein were analyzed for H_2O_2 formation and measured calorimetrically at 540nm. Results were converted using the standard curve for a known concentration of H_2O_2 and expressed in micromolar.

Nitrate/nitrite concentration

The concentrations of nitrite/nitrate were measured in tissue homogenates (ZSF1-HFPEF:n=10, ZSF1-Ctrl:n=10, AS:n=16; HFpEF:n=16; HFrEF:n=16) by means of a colorimetric assay kit (BioVision). This kit uses a two-step protocol. First, nitrate is

converted to nitrite using nitrate reductase. Subsequenlty Griess Reagents convert nitrite to an azochromophore reflecting NO concentration in the tissue and plasma samples. Nitrite levels can be measured independently from nitrate by omitting the first step.

Immunoelectron microscopic quantification of 3-nitrotyrosine

A standard pre-embedding immunogold electron microscopy protocol was used in this study. Briefly, cardiac samples (ZSF1-HFpEF:n=6, ZSF1-Ctrl:n=6;) were fixed in 4% paraformaldehyde, 15% saturated picric acid in 0.1M phosphate buffer pH 7.4. Sections were cut on a vibratome (Leica VT 1000S) for a thickness of 50µm, blocked in 20% NGS (Vector Laboratories) in PBS and were incubated with Nitrotyrosin (Millipore 06-284) primary antibody in phosphate-buffered saline containing 5% NGS. After washing, sections were incubated with 1.4nm gold-coupled secondary antibodies (Nanoprobes). After several washes sections were postfixed in 1% glutaraldehyde in PBS and then incubated with HQ Silver kit (Nanoprobes). After treatment with OsO4, sections were stained with uranyl acetate, dehydrated and at embedded in Durcupan resin (Fluka). Ultrathin sections were prepared (Ultracut S) and examined with a ZEISS LEO 910 electron microscope. Images were subsequently analyzed with Slidebook (3i). 3-Nitrotyrosine expression was calculated as the sum of 3-nitrotyrosine gold-labelling area related to the total area of cardiomyocytes or endothelium.

Myocardial PKA, PKC, PKG, cGMP and CaMKII activity

All kinase activities were assessed in myocardial homogenates. Activities (ZSF1-HFpEF:n=10, ZSF1-Ctrl: n=10) were analyzed as described previously for PKA and PKC (17) and for PKG and cGMP (18).

For CaMKII, activity was determined using a CycLex® CaMKII assay kit (CY-1173; MBL Corporation, MA) according to the manufacturer's guidelines (ZSF1-HFpEF:n=10, ZSF1-Ctrl:n=10;).

Statistical analysis

Differences between groups were analyzed by one-way ANOVA followed by Bonferroni-adjusted t tests. Single comparisons were assessed by an unpaired Student t test. All analyses were performed using Prism software (GraphPad Software Inc, version 6.0).

JACC: HEART FAILURE
VOL. 4, NO. 4, 2016

ISSN 2213-1779/$36.00
PUBLISHED BY ELSEVIER
http://dx.doi.org/10.1016/j.jchf.2015.11.013

EDITORIAL COMMENT

Inflammation in Heart Failure With Preserved Ejection Fraction

Time to Put Out the Fire*

Mardi Gomberg-Maitland, MD, MSc,[a] Sanijv J. Shah, MD,[b] Marco Guazzi, MD, PhD[c]

Heart failure with preserved ejection fraction (HFpEF) is a common and costly condition associated with a high frequency of comorbid conditions. HFpEF prevalence is rising compared to heart failure with reduced ejection fraction (HFrEF), without any change in clinical outcomes over the past 20 years (1).

In contrast to HFpEF, HFrEF outcomes have improved with the advent of multiple drug therapies. Most of the therapeutic approaches proven to be effective in HFrEF have been tested and developed in controlled experimental studies in animal models (2) by dissecting the role of abnormal signaling in intracellular molecular pathways (3). The most impressive examples come from studies on angiotensin-converting enzyme inhibitors and beta-blockers. Mechanistic research enabled appropriate therapeutic targets and favored the development of genetically manipulated small animal strains (3).

Thus far, therapeutic remedies have been ineffective in HFpEF likely because a multitude of phenotypes are grouped under the same definition (4). Another central reason for the lack of therapies for HFpEF may be related to the erroneous assumption that the therapeutics approved for treating HFrEF can be successfully transposed to HFpEF without a full appreciation of differences in cardiac adaptation and extent of diastolic impairment (5) or, more simply, without taking full advantage of translational science and appropriate animal models. Indeed, animal models of HFpEF are not as well established as many capture components of specific hemodynamic aspects, such as left ventricular (LV) vascular uncoupling (6), left atrial dysfunction, and pulmonary hypertension (7), but poorly reproduce the integrative complexity of human disease and related comorbidities such as obesity, diabetes, chronic kidney disease, and atrial fibrillation.

A systemic inflammatory state is central to these common comorbidities associated with HFpEF and oxidative stress and endothelial dysfunction are prominent features that characterize the so-called metabolic risk, especially in the presence of obesity (8). It is noteworthy that occurrence of an inflammatory activation is predictive of incident HFpEF but not HFrEF (9). Once exposed to inflammatory activation, the cardiac myocyte suffers from an impaired cellular signaling at a variety of levels. Specifically, endothelial dysfunction in the coronary microcirculation may alter the paracrine cross-talk signaling between coronary circulation and cardiomyocyte through decreased bioavailability of nitric oxide (NO) and its downstream cyclic guanosine monophosphate (cGMP) protein kinase G (PKG) pathway (10). Collagen turnover and titin homeostasis critically depend on cGMP and PKG signaling, which is absolutely relevant for passive properties (stiffness) of the LV, as demonstrated in animals, isolated human cardiomyocyte preparations (11,12), and the intact human myocardium (13). Recent research suggests that coronary microvascular endothelial inflammation is

*Editorials published in *JACC: Heart Failure* reflect the views of the authors and do not necessarily represent the views of *JACC: Heart Failure* or the American College of Cardiology.

From the [a]Cardiology Section, Department of Medicine, University of Chicago, Chicago, Illinois; [b]Division of Cardiology, Northwestern University Feinberg School of Medicine, Chicago, Illinois; and the [c]Cardiology Department, University of Milan, I.R.C.C.S. Policlinico San Donato, San Donato Milanese, Milan, Italy. Dr. Shah has received research grant support from the National Institutes of Health (R01 HL107557 and R01 HL127028), Actelion, and Novartis; and has served as a consultant for AstraZeneca, Bayer, and Novartis. All other authors have reported that they have no relationships relevant to the contents of this paper to disclose.

also associated with coronary microvasculature rarefaction, with a resultant reduction in capillary density that may impair coronary flow reserve, thereby causing LV systolic and diastolic dysfunction (14). According to this emerging evidence, inflammatory activation and its multisignaling cascade of events on the coronary microvasculature and myocardium is increasingly recognized as a primary contributor in the pathogenesis of HFpEF, and thus has become an intriguing target for intervention (15).

SEE PAGE 312

In this issue of *JACC: Heart Failure*, Franssen et al. (16) provide further demonstration of the putative role of myocardial microvascular inflammation in HFpEF by studying its effects on cardiac myocyte oxidative stress and NO pathway signaling in a parallel human and animal study. The authors designed an elegant study that included analysis of myocardial biopsies from a group of patients with increased body mass index and left ventricular hypertrophy (LVH) associated with HFpEF and 3 comparison groups: nonobese HFrEF, aortic stenosis, and control groups. The results of the human study were compared with findings obtained in 2 strains of ZSF1 rats—one leptin resistant, obese, hypertensive, and diabetic and the other nonobese, nondiabetic, and hypertensive. The ZSF1 leptin-resistant model develops LVH and signs of HF, increased LV filling pressure, myocyte stiffness, and congestion, with preservation of LV ejection fraction.

The authors found a similar inflammatory phenotype in HFpEF patients and ZSF1 obese rats, with the same expression of adhesion molecule (ICAM-I, E-selectin), oxidative stress (increased H_2O_2 and

FIGURE 1 Proposed Iterative Testing With Animal Models and Human T1 Mechanistic Phase Trials for the Development of Novel Therapies for Heart Failure With Preserved Ejection Fraction

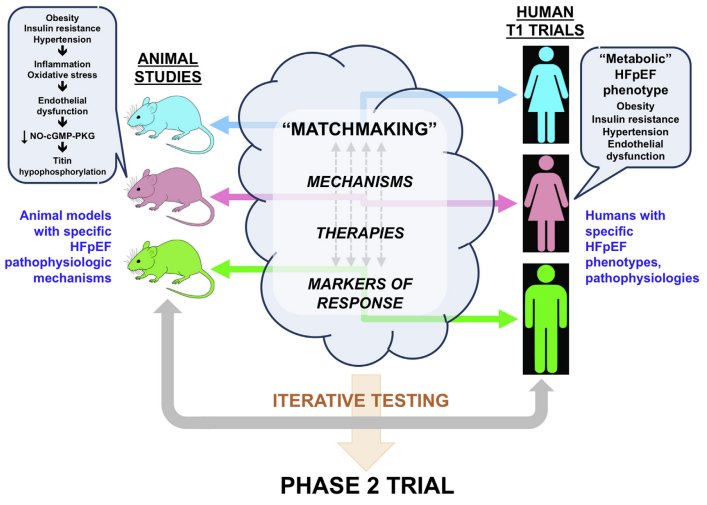

Iterative testing of novel therapies on the basis of matching of animal models, molecular mechanisms, therapies, markers of treatment response, and humans with specific heart failure with preserved ejection fraction (HFpEF) phenotypes. Matching of animal models, molecular mechanisms, targeted therapies, markers of treatment response, and specific HFpEF phenotypes may lead to improved results in HFpEF clinical trials. For example, iterative testing with the ZSF1-HFpEF rat and patients with the metabolic HFpEF phenotype may provide a platform for the evaluation of therapies that specifically target deficiencies in the nitric oxide-cyclic guanosine monophosphate-protein kinase G (NO-cGMP-PKG) pathway.

reduced nitrite/nitrate concentration), and evidence of uncoupling of endothelial NO synthase. Findings typical of the HFpEF phenotype were not present in the HFrEF and aortic stenosis biopsy samples.

The HFpEF human "metabolic phenotype" adopted in this study was highly selected (body mass index >30 kg/m^2, hypertension, and diabetes) reproducing the most frequent constellation of comorbid disorders in HFpEF (17). Compared to previous observations by the same group (18) the findings of the present study have been extended to a wider characterization of molecular arrays, particularly the multilevel examination of microvascular inflammation, oxidative stress, NO-cGMP-PKG signaling, and titin analysis. The more extensive characterization of the molecular cascade allows us to draw solid conclusions on the associative and, in part, mechanistic role of these pathways in the context of the human HFpEF syndrome.

Because HF is by definition a syndrome with sign and symptoms of congestion, a full characterization of congestive state in both human and animals would have been useful especially considering that the patients included in the present study were hospitalized for an acute episode of decompensated HF whereas the rats that were studied had a more chronic, progressive congestive state. On the basis of the results of the study, these differences in the human subjects versus animal models do not appear relevant in terms of inflammatory activation; however, on the basis of the association of inflammatory markers such as C-reactive protein with the severity of LV end-diastolic pressure increases in HF (19), documentation of the severity of congestion in the patients and the animals in the study could have assisted with understanding whether the authors' results were more applicable to a more advanced stage of HFpEF.

The study by Franssen et al. (16) also could have benefited from a more detailed analysis of cardiac structure and function; indices such as degree of LVH, type of remodeling, and cardiac mechanics were lacking both in the humans and animal models included in the study. How much passive stiffness is affected by inflammatory activation per se rather than pressure overload and ventricular-vascular uncoupling in the in vivo setting remains an unanswered question.

Why is this study important and how do these parallel human and basic science analyses enhance knowledge in the field? The study not only elucidates potential causative metabolic processes but also helps us as clinical investigators better design clinical trials. Limiting our early-phase HFpEF therapeutic trials to patients with only certain comorbidities, similar to these animal models, may result in a more targeted clinical trial approach with early mechanistic studies in limited numbers of patients (i.e., T1 phase trials). An iterative, nimble exchange between animal studies and T1 human studies could result in more fruitful phase 2 and 3 HFpEF clinical trials (**Figure 1**). If successful this type of strategy would also help validate the use of specific animal models for HFpEF. Despite a few drawbacks, the findings by Franssen et al. (16) remain meritorious because they add evidence to the emerging prominent role of inflammatory activation in HFpEF and recall the necessity to optimize the bench to bedside methodological gaps at a level equivalent to what has been successful for HFrEF (i.e., establish animal models that may accurately reproduce the cellular pathways closest to the specific human failing heart phenotype and associated comorbidities). These emerging perspectives and an extended profiling of the cGMP-PKG signaling cascade seem preparatory to appropriately match anti-inflammatory therapeutic interventions to the "inflamed" HFpEF phenotype in large-scale clinical trials.

REPRINT REQUESTS AND CORRESPONDENCE TO: Dr. Mardi Gomberg-Maitland, Section of Cardiology, University of Chicago, 5841 South Maryland Avenue, MC 5403, Chicago, Illinois 60611. E-mail: mgomberg@bsd.uchicago.edu.

REFERENCES

1. Gerber Y, Weston SA, Redfield MM, et al. A contemporary appraisal of the heart failure epidemic in Olmsted County, Minnesota, 2000 to 2010. JAMA Intern Med 2015;175:996-1004.

2. Braunwald E. The war against heart failure: The lancet lecture. Lancet 2015;385:812–24.

3. Patten RD, Hall-Porter MR. Small animal models of heart failure: development of novel therapies, past and present. Circ Heart Fail 2009;2:138–44.

4. Shah SJ, Katz DH, Selvaraj S, et al. Phenomapping for novel classification of heart failure with preserved ejection fraction. Circulation 2015;131:269–79.

5. Katz AM, Rolett EL. Heart failure: when form fails to follow function. Eur Heart J 2015 Oct 24 [E-pub ahead of print].

6. Takimoto E, Champion HC, Li M, et al. Chronic inhibition of cyclic gmp phosphodiesterase 5a prevents and reverses cardiac hypertrophy. Nat Med 2005;11:214–22.

7. Chen Y, Guo H, Xu D, et al. Left ventricular failure produces profound lung remodeling and pulmonary hypertension in mice: Heart failure causes severe lung disease. Hypertension 2012;59:1170–8.

8. Wohlfahrt P, Redfield MM, Lopez-Jimenez F, et al. Impact of general and central adiposity on ventricular-arterial aging in women and men. J Am Coll Cardiol HF 2014;2:489–99.

9. Kalogeropoulos A, Georgiopoulou V, Psaty BM, et al. Inflammatory markers and incident heart failure risk in older adults: the Health ABC (Health, Aging, and Body Composition) study. J Am Coll Cardiol 2010;55:2129–37.

10. Paulus WJ, Tschope C. A novel paradigm for heart failure with preserved ejection fraction: comorbidities drive myocardial dysfunction and remodeling through coronary microvascular endothelial inflammation. J Am Coll Cardiol 2013;62:263-71.

11. Borbely A, van der Velden J, Papp Z, et al. Cardiomyocyte stiffness in diastolic heart failure. Circulation 2005;111:774-81.

12. Bishu K, Hamdani N, Mohammed SF, et al. Sildenafil and b-type natriuretic peptide acutely phosphorylate titin and improve diastolic distensibility in vivo. Circulation 2011;124:2882-91.

13. Zile MR, Baicu CF, Ikonomidis JS, et al. Myocardial stiffness in patients with heart failure and a preserved ejection fraction: contributions of collagen and titin. Circulation 2015;131:1247-59.

14. Mohammed SF, Hussain S, Mirzoyev SA, et al. Coronary microvascular rarefaction and myocardial fibrosis in heart failure with preserved ejection fraction. Circulation 2015;131:550-9.

15. Lim SL, Lam CS, Segers VF, et al. Cardiac endothelium-myocyte interaction: Clinical opportunities for new heart failure therapies regardless of ejection fraction. Eur Heart J 2015;36:2050-60.

16. Franssen C, Chen S, Unger A, et al. Myocardial microvascular inflammatory endothelial activation in heart failure with preserved ejection fraction. J Am Coll Cardiol HF 2016;4:312-24.

17. Ferrari R, Bohm M, Cleland JG, et al. Heart failure with preserved ejection fraction: uncertainties and dilemmas. Eur J Heart Fail 2015;17:665-71.

18. van Heerebeek L, Hamdani N, Falcao-Pires I, et al. Low myocardial protein kinase g activity in heart failure with preserved ejection fraction. Circulation 2012;126:830-9.

19. Shah SJ, Marcus GM, Gerber IL, et al. High-sensitivity c-reactive protein and parameters of left ventricular dysfunction. J Card Fail 2006;12:61-5.

KEY WORDS heart failure preserved ejection fraction, Inflammation